Soil Moisture Variations in Frozen Ground Subjected to Hydronic Heating

Svein-Erik Sveen[1]; Hung Thanh Nguyen[2]; and Bjørn Reidar Sørensen[3]

Abstract: Full-scale thawing experiments, performed on three types of homogenous, initially frozen soils, were carried out during late winter 2011 and repeated in 2012. An auxiliary heat source (hydronic heating) was employed to initiate and expedite the thawing process. The corresponding phase change, soil temperature increase, and variations in bound and unbound water content were monitored during the experiments. The resulting thermal response have been published in an earlier paper by the authors. In the current paper, the remaining results are presented. This includes spatial and temporal soil moisture variations and resulting thaw rates. Results from both experiments show similar trends. Generally, frost-susceptible soils, such as silty sand, contain more water and thaw slower relative to coarser soils, such as gravelly sand. Very porous soils (uniform gravel) with low water content thaw comparatively slower. Thaw rates compiled from soil moisture records correspond well with similar based on soil temperature. The degree of water redistribution and migration is higher in silty sand compared with coarser soils. These processes are more prominent in the uppermost layer for all soils examined.
DOI: 10.1061/(ASCE)CR.1943-5495.0000231.

Author keywords: Artificial thawing; Frozen ground; Soil water content; Phase change; Ground temperature; Performance characteristics.

Introduction

Frozen ground engineering has developed rapidly in the past several decades under the pressure of necessity. As frozen soils-related problems have broadened in scope, the inadequacy of earlier methods for dealing with them have become increasingly apparent (Andersland and Ladanyi 2004). This is evident when observing how artificial thawing techniques and soil monitoring methods have evolved over the years. Artificial thawing is a prerequisite to frozen ground engineering in regions experiencing seasonal frost or permafrost. Esch (2004) gives examples of various methods in a historical perspective, such as steam thawing, hot- and cold-water thawing, and electric thawing, all of which came with the mechanization of mine workings in the early 1900s. While some of these methods saw some development over the years, none of them were widely used. That changed with the introduction of defrosting systems based on hydronic or water-borne heat two decades ago. Since then, the applicability and efficiency of the method have been further improved, promoting widespread use in cold regions (Heatwork 2016a; Wacker Neuson 2016).

As opposed to traditional techniques, hydronic thawing utilizes conduction as the main heat transfer mechanism. Flexible hot-water pipes are laid out on the frozen ground surface in order to rapidly thaw the underlying soil, as shown in Fig. 1. During operation, the pipes are covered with combined vapor and insulation blankets.

As reported in an earlier paper by the authors (Sveen et al. 2016), this method is capable of thawing 1 m of gravelly sand in approximately 3.5 days, silty sand in about four days, and uniform gravel in approximately 11.5 days. The results reported in the present paper is a continuation of the data obtained from Sveen et al. (2016). The thaw rates generally decrease with increasing depth or distance to the heat source, varying from 22–37 cm/day after one day to 12–24 cm/day after six days of continuous thawing. The trend is similar for natural thawing, but then at considerably lower thaw rates. Obviously, the increased thaw efficiency is primarily related to the additional thermal energy provided by the defrosting system. Another important difference is that natural thawing typically affects large areas, which allows for lateral water transport (Guan et al. 2010a, b; Kurylyk et al. 2014), whereas artificial thawing is limited to small areas where excess water becomes trapped, thus promoting the thawing process (Baladi et al. 1981).

It is commonly known that the type of soil and quantity of ice or water greatly influence on the rate and depth of thaw. An early field study in Point Barrow, Alaska, by Drew et al. (1958) found that Arctic brown soil thawed earlier in the spring, to a greater depth, and froze earlier in the autumn compared with adjacent poorly drained areas. In a review of fundamental analytical and numerical solutions for heat transfer in thawing soils by Nixon and McRoberts (1973), they showed that the total quantity of water that changes phase is one of the dominant factors affecting the thawing of frozen soils. This is supported by a number of more recent studies based on laboratory and field experiments (Simonsen and Isacsson 1999; Bäckström 2000; Nassar et al. 2000; Yang et al. 2003; Xu and Spitler 2014).

In comparison to abundant studies on frost penetration and artificial freezing, investigations of the opposite phenomena are scarce. Considering the recent development within hydronic thawing and efforts made to further improve the method, there is a need for

[1]Associate Professor, UiT-Norwegian Arctic Univ., Faculty of Engineering Science and Technology, Institute of Building, Energy and Material Technology, P.O. Box 385, N-8505 Narvik, Norway (corresponding author). ORCID: https://orcid.org/0000-0001-9158-1653. Email: svein-erik.sveen@uit.no

[2]Associate Professor, UiT-Norwegian Arctic Univ., Faculty of Engineering Science and Technology, Institute of Building, Energy and Material Technology, P.O. Box 385, N-8505 Narvik, Norway. Email: hung.thanh.nguyen@uit.no

[3]Professor, UiT-Norwegian Arctic Univ., Faculty of Engineering Science and Technology, Institute of Building, Energy and Material Technology, P.O. Box 385, N-8505 Narvik, Norway. Email: bjorn.r.sorensen@uit.no

Note. This manuscript was submitted on February 5, 2017; approved on July 6, 2020; published online on September 10, 2020. Discussion period open until February 10, 2021; separate discussions must be submitted for individual papers. This paper is part of the ***Journal of Cold Regions Engineering***, © ASCE, ISSN 0887-381X.

more performance data. That was part of the motivation for establishing an outdoors Frost in Ground laboratory (FiG-lab) in 2007. The first full-scale thawing experiments on various types of homogenous soils were performed in March the same year, with preliminary results published in 2010 (Myhre 2010; Sveen and Sørensen 2010). During 2009–2010, the FiG-lab was relocated and upgraded with soil moisture monitoring capabilities among other improvements. The present study is the first to benefit from access to the new lab facilities (Sveen and Sørensen 2013). Thawing experiments on three types of soils were carried out during the winter of 2011 and repeated in 2012. In particular, the investigation was designed to evaluate performance characteristics of the hydronic method used for thawing of frozen ground. A defrosting system based on this principle was used to provide the heat necessary for artificial thawing. The resulting phase change, soil temperature increase, and variation in water content for each soil type were monitored during the process.

The thermal response and associated thaw rates from both experiments have been published in a previous paper (Sveen et al. 2016), together with a description of the hydronic thawing method. The results from both winter seasons showed similar trends, with comparable and considerable higher thaw rates for well-graded sand and silty sand compared with crushed gravel. In the current paper, the remaining results are presented. Specifically, this includes soil moisture variations with depth and time occurring in three types of initially frozen soils, and resulting thaw rates based on soil moisture records. Maximum levels of soil water content during thawing are compared with levels occurring after a period of continuous thawing. The results from both winter seasons are compared. In addition, basic information about the FiG-lab and instrumentation are presented.

Methodology

This study is based on two separate, full-scale experiments performed in April 2011 and March 2012 at the FiG-lab (N68° 26′55″, E17°31′16″), located about 6 km east-northeast of Narvik, Norway. Three types of soils were exposed to the elements, and thus allowed to freeze naturally during late autumn and winter, before being artificially thawed. An external heat source based on hydronic heat was employed to initiate and expedite the process. Relevant operation parameters of the heat source, as well as soil temperatures and soil moisture levels, were monitored during the experiments. The preparations made, procedures followed, and defrosting systems used were identical for both experiments. While a full description of the new lab facilities and supplementary information is given in Sveen and Sørensen (2013), key points are repeated in the following sections for clarity.

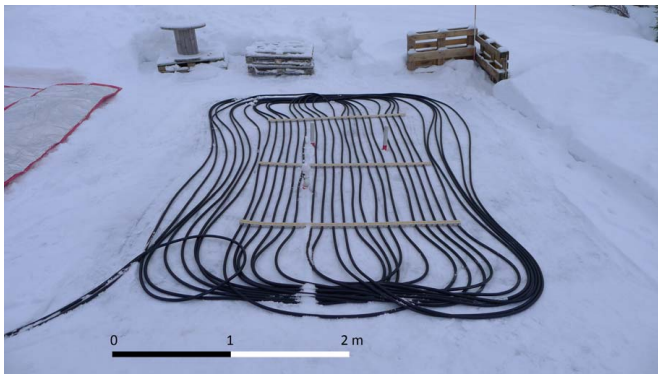

Fig. 1. (Color) An overview showing hot-water pipes laid out on frozen gravel, before being covered with insulation blankets, February 29, 2012. In this particular case, the pipes covers an area of approximately 3.5 × 4.5 m. (Image by Svein-Erik Sveen.)

Heat Load

The main components and principle of operation are described in detail in Sveen et al. (2016). An oil burner provided heat to the water–glycol mixture contained in the boiler. A pump ensured circulation of the hot fluid through flexible rubber pipes connected to a distribution manifold attached to the boiler. The manifold divided the flow evenly between up to three pipes, thus allowing for single-, dual-, or triple-pipe operation. During thawing, the pipes were covered with combined vapor barrier and insulation blankets to reduce heat losses from radiation and convection. Typical horizontal spacing between pipes was 5–40 cm.

The unit used in this study was a 50-L boiler heated by an oil burner of 103 kW gross capacity ($\dot{W}_{\text{gross}}$). Three distribution pipes were available, each 210 m in length, outer diameter of 24 mm, and holding approximately 42 L of fluid. The boiler temperature was set manually up to 100°C by a thermostat. During startup, the burner ran at full capacity (continuously) until the desired set-temperature was reached.

Accounting for the fuel flow rate (8.30 L/h), net calorific value of the type of fuel was used (9.96 kW·h/L) and the theoretical maximum burner efficiency (0.94) (Heatwork 2016b), the maximum heat transfer rate to the boiler ($\dot{W}_{\text{max}}$) became 77.7 kW. As the temperature of the frozen ground surface increased and the thawing progressed, the temperature difference between the fluid supplied by the boiler and the fluid returning began to decline. From there on, the burner began running intermittently, resulting in a gradually lower fuel consumption with time. In practical terms, this implies that the system delivered a transient heat load. In this study, seen over a period of 12 days of thawing using all three pipes, the mean heat transfer rate ($\dot{W}_{\text{mean}}$) was approximately 33 kW.

Test Arrangement

The FiG-lab is situated at a flat area, approximately 140 m above sea level on the northern slope of a hillside, about 3 km northwest

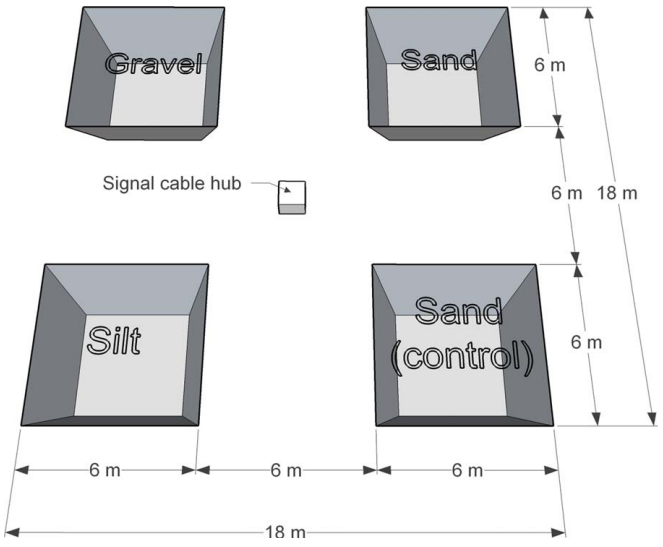

Fig. 2. Overview of the Frost in Ground laboratory soil-bin arrangement. (Reprinted from Sveen et al. 2016, © ASCE.)

of the mountain Rombakstøtta (1,230 m). The secluded location makes it less exposed to solar radiation. The uppermost 3 m at the site was replaced with moraine gravel. Within an area extending 18 × 18 m, four 6 × 6 m soil-bins were established in a quadratic pattern, as shown in Fig. 2. Meltwater during spring thaw is lead outside or under the prepared area through buried pipelines.

The existing soil of each bin was exchanged with homogenous soil samples: gravelly sand, silty sand, and 8–22 mm uniform, crushed gravel. The additional sand (control) bin was included to ensure the integrity of the bins actually being thawed during the experiments. There was no physical barrier separating the soil samples from the adjacent soil, except for a thin, permeable membrane in the gravel bin.

All four bins were fitted with an identical array of soil temperature and soil moisture sensors, located at the center of each bin. The sensors extended to 1.8 m depth along four vertical axes, covering a 1 × 1 m horizontal area. During the two-week thawing experiments in April 2011 and March 2012, soil temperature and water content in all bins were recorded every hour using thermocouples, thermistor strings, resistance blocks, and capacitance moisture probes. In addition, fuel consumption, pipe-flow rates, and fluid temperatures of the hydronic defrosting system were monitored at similar intervals.

The vertical alignment of the various sensors was ensured by mounting them to a custom-made frame. The vertical spacing between the thermocouples was 0.1 m, starting at the ground surface level and ending at 1.5 m depth, with an additional thermocouple at 1.8 m. The remaining groups of sensors (including soil moisture) were placed at 0.2 m intervals, starting from 0.1 m below ground surface and ending at 1.8 m depth. Consequently, they were aligned with every second thermocouple. The sensor frames extended 2.16 m vertically and covered a 1 × 1 m horizontal area at the center of each soil bin. Signal cables leading from the bins were collected at a central hub, from where the cables were led to a cabin sheltering the monitoring systems.

After both experiments (during autumn), soil samples were collected from each bin for determination of grain-size distribution, porosity, initial moisture content, and dry density. Ambient air conditions and precipitation were gathered from a nearby meteorological station maintained by the Norwegian Meteorological Institute (NMI) during both winter seasons.

Soil Moisture Monitoring

Soil moisture content was monitored using Sentek EnviroSCAN capacitance-based sensors (Sentek Environmental Technologies, Kent Town, South Australia) installed in customized access tubes, and by Watermark 200SS electrical resistance sensors embedded in the soil (Irrometer Co., Inc., Riverside, California). The former is an electromagnetic sensor that indirectly measures volumetric water content (θ_v) based on the relative permittivity or apparent dielectric constant (K_a) of the various constituents of the surrounding soil, shown in Fig. 3(b). The latter measures soil water tension or suction, based on the resistance across two electrodes inside a resistance-block embedded in the soil, as shown in Fig. 3(a).

Capacitance-based monitoring is commonly referred to as frequency-domain reflectometry (FDR) because it applies an oscillating voltage to measure the capacitance and thus the dielectric permittivity of the surrounding medium. The soil medium can be represented as a four-component dielectric mixture of air, solids, bound water, and free water, all of which have different dielectric constants. A substance's K_a is defined as the ratio of its dielectric permittivity to that of free space, and is not constant, but varies with the frequency of the sensor (Rudnick et al. 2015). At radio

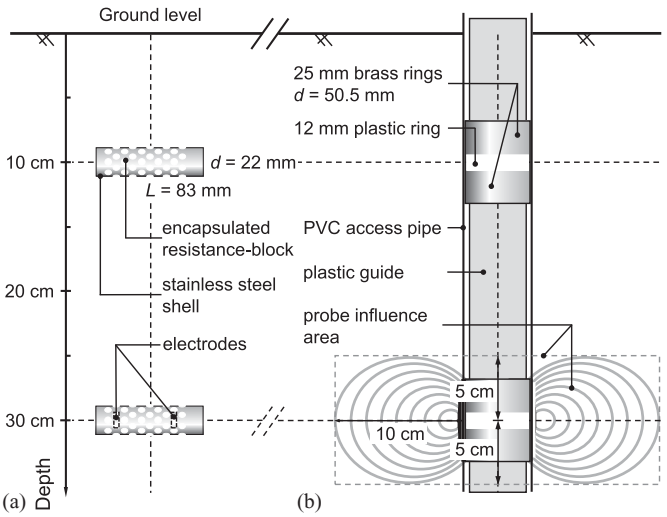

Fig. 3. Illustration showing the two types of soil moisture sensors used and their vertical spacing near the ground surface: (a) Watermark model 200SS electrical resistance-blocks; and (b) Sentek EnviroSCAN capacitance sensors.

frequencies, the dielectric constant of pure water at 20°C and atmospheric pressure is about 80, that of soil solids is 3–5, and that of air is 1 (Evett and Steiner 1995). Consequently, the overall dielectric constant of the soil is largely dependent on the soil's water content.

The normalized capacitance sensor output (scaled frequency) is converted to θ_v (vol%) using a default calibration equation representative for a range of different soils. The sensor oscillation frequency is set sufficiently high (~100 MHz) to avoid interference from saline soil water. Temperature effects are negligible for soil temperatures ranging from 10°C to 30°C (Paltineanu and Starr 1997). The axial range of influence is 100% within 5 cm above and below the center of the sensor, as indicated in Fig. 3(b). The overall radial range of influence extends 18 cm from the access pipe surface, but where almost all (99%) of the sensor's response is obtained within the first 10 cm.

Electrical resistance-blocks are commonly used for estimation of soil moisture status and irrigation scheduling (Spaans and Baker 1992). The underlying principle is that the electrical resistance of the matrix changes as the water content of the block changes.

Since it exchanges water with the surrounding soil, the block's output can be attributed to soil moisture status. Given a known relationship between electrical resistance and water potential of the matrix, the soil's matrix potential (Ψ_m) can be determined. The sensor consists of two electrodes, a resistance-block and membrane, held in place by a perforated stainless-steel shell that prevents the reference material from dissolving over time and protects against commonly found soil water salinity levels. The output voltage is proportional to the resistance in the porous matrix and is converted to Ψ_m (kPa) by a default calibration equation (Shock et al. 1998), ranging from −10 to −75 kPa. The results are temperature compensated.

According to the manufacturers, both sensors are capable of operating under frozen ground conditions. In such circumstances, the Sentek sensor only reacts to bound soil water, that is, the unfrozen water film bound to the surfaces of the solids. It will not respond to frozen pore water, since the dielectric properties of ice is different from unbound (free) water. The Watermark sensor interprets frozen soil as regular soil being completely dry. Consequently, the resulting resistance will be very high compared with that in thawed soil where it is close to zero.

Results

The following sections present details about the soils tested, weather conditions, and soil moisture records from the experiments performed in 2012 and 2011. To ensure conformity and make it easier to compare with the temperature records presented in Sveen et al. (2016), the soil moisture datasets from 2012 are presented before those from 2011, instead of chronologically.

Soils Tested

According to the Unified Soil Classification System (Andersland and Ladanyi 2004), the materials used in the experiments are characterized as coarse-grained soils and grouped as gravelly sand (SP), sand–silt mixture (SP–SM), and poorly graded gravel (GP), as presented in Table 1. In context, coarse-grained means that more than half of the material (by weight) is finer than 75 mm and larger than 0.075 mm. The listed dry densities are the average of three soil samples per bin.

Fig. 4 shows the grain-size distribution curves (GSDs) for the soils used, together with the effective diameter (D_{10}), the coefficient of uniformity (C_u), and the coefficient of curvature (C_c) for sand. In order for the sand to be classified as well graded (SW), less than 5% of the material must be smaller than 0.075 mm (fines), C_u must be greater than 6, and C_c must be between 1 and 3. Since sand only meets two of three criteria, it is classified as poorly graded (SP). Similarly, in order for silty sand to be classified purely as SM (sand–silt mixture), it must have more than 12% fines. Since it has less than that, but still more than 5%, it is classified as a borderline case, designated SP–SM.

Gravel is classified as poorly graded (GP) as the material is predominantly within 8–22 mm. In the following it is termed as "uniform" or "uniform, crushed" gravel since it is supplied from a local quarry where the manufacturer uses heavy machinery to crush bedrock and portion it out into commonly used fractions.

Initial values for water and ice content do not exist, as frozen soil cores were not collected prior to thawing owing to lack of access to suitable sampling equipment.

Weather Conditions

Records of daily mean, high, and low air temperature and precipitation prior to and during the experiments are collected from an official weather station maintained by the NMI. The station is located at Straumsnes, about 5.5 km east of the FiG-lab, 200 m above sea level. Referring to NMI's long-term climate normal (30-year average), mean annual air temperature, frost index, and precipitation for a normal year in Narvik is 3.8°C, roughly 9,000 h°C (degree hours), and 855 mm, respectively. The cold season for the region is five months, lasting from the beginning of November to the end of March.

According to public records from NMI covering January–February 2012, the weather conditions were characterized by slightly higher air temperatures and less precipitation compared with the previous year. There was almost no precipitation, and consequently moderate snow cover (<25 cm), until February 10. The snow cover stayed the same until the last week of February, during

Table 1. Soil classification, dry density, and volumetric water content

	Unified soil classification			Volumetric water content (vol%)	
Soil bin	Group	Description	Dry density (kg/m^3)	2012	2011
A[a]	SP	Gravelly sand (33.4% gravel, 62.9% sand, 3.7% fines)	1,790	6.4[b]	18.4[c]
B				11.0	11.1
C	SP-SM	Sand-silt mixture (16.3% gravel, 76.6% sand, 7.1% fines)	1,727	10.6	11.3
D	GP	Poorly graded gravel (98.9% gravel, 0.7% sand, 0.4% fines)	1,446	2.7	2.9

Note: Volumetric water content are the average of nine soil moisture sensors per bin (0.1–1.8 m depth) 12 days into each thawing experiment, March 20, 2012, and April 21, 2011, respectively.
[a]Control bin, monitored, but not affected by thawing.
[b]Average reading in frozen soil.
[c]Average reading in naturally thawed soil.

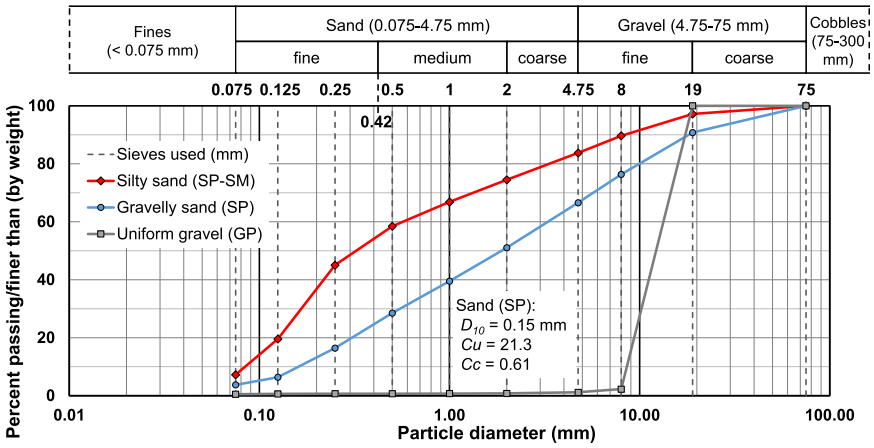

Fig. 4. (Color) Grain-size distribution curves (group classification in parenthesis) for the types of soils used in the experiments. The effective diameter (D_{10}), coefficient of uniformity (C_u), and coefficient of curvature (C_c) applies only to sand (SP).

J. Cold Reg. Eng., 2020, 34(4): 04020025

which it increased to about 60 cm. At that time, it was removed as a part of the preparations for the fieldwork.

Detailed charts of weather conditions during the experiments are shown in Sveen et al. (2016). Mean air temperature during the period of artificial thawing (March 8–23) was 0.1°C. Daily average precipitation was 3.8 mm, mainly as snow. According to thermocouple records for silty sand, the frost depth was 1.4–1.5 m. For gravelly sand, it was between 1.5 and 1.8 m, and for uniform gravel more than 1.8 m.

Similarly, NMI records covering January–March 2011 show slightly lower air temperatures and more precipitation in general compared with the same period in 2012. There was no snow cover until January 27, increasing to about 70 cm in mid-February. It varied between 50 and 80 cm up to one week prior to the experiments, when it was removed as part of the preparations. As opposed to 2012, there were several warm spells in the month leading up to the fieldwork, combined with precipitation in the form of rain or sleet.

According to thermocouple records for silty sand from 2011, the ground was frozen at 1.1–1.2 m depth. For gravelly sand and uniform gravel, the frost depth was about 1.5 m. Mean air temperature during the experiments (April 9–21) was 2.8°C and average precipitation 4.8 mm per day, mainly as rain and sleet.

Soil Moisture Profiles

The following two sections contain records of volumetric water content (Figs. 5 and 6) and soil matrix potential (Figs. 7 and 8) from both thawing experiments. The latter are determined from the measurements of electrical resistance. Datasets from 2012 are presented before those from 2011 for easy comparison to the previous paper (Sveen et al. 2016). The soil temperature records in the previous paper cover the time period from 2 PM March 8 to 2 PM March 21, 2012, and 10 AM April 9 to 6 PM April 21, 2011, respectively. Temperature data is missing for the initial 17 h from the experiment in 2011. These periods correspond to the time where artificial thawing was occurring, that is, when the defroster was running. However, the soil moisture records presented in the current paper from the same time periods cover the full day (24 h) at the start and end dates.

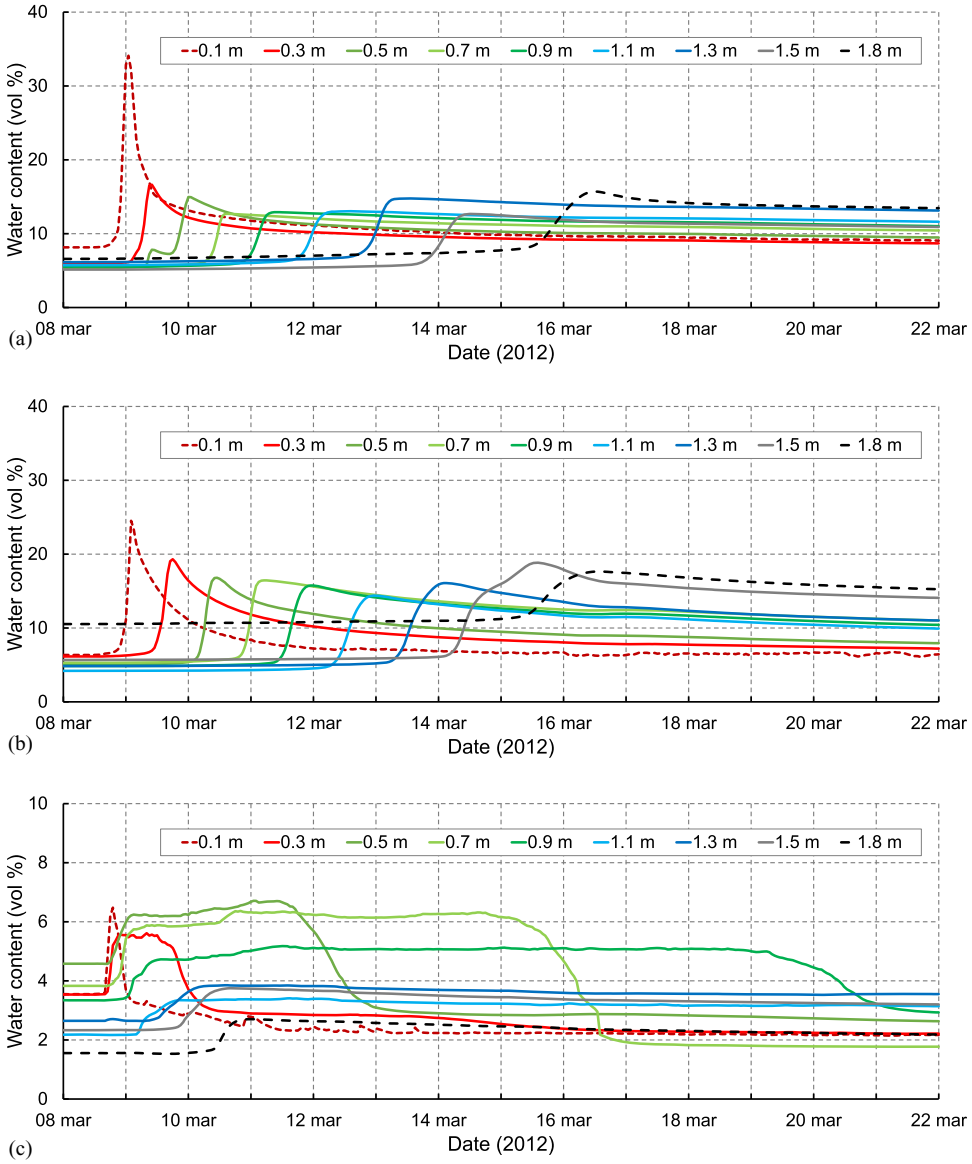

Fig. 5. (Color) Volumetric water content based on Sentek EnviroSCAN capacitance sensors in homogenous: (a) gravelly sand; (b) silty sand; and (c) 8–22 mm uniform, crushed gravel, March 2012.

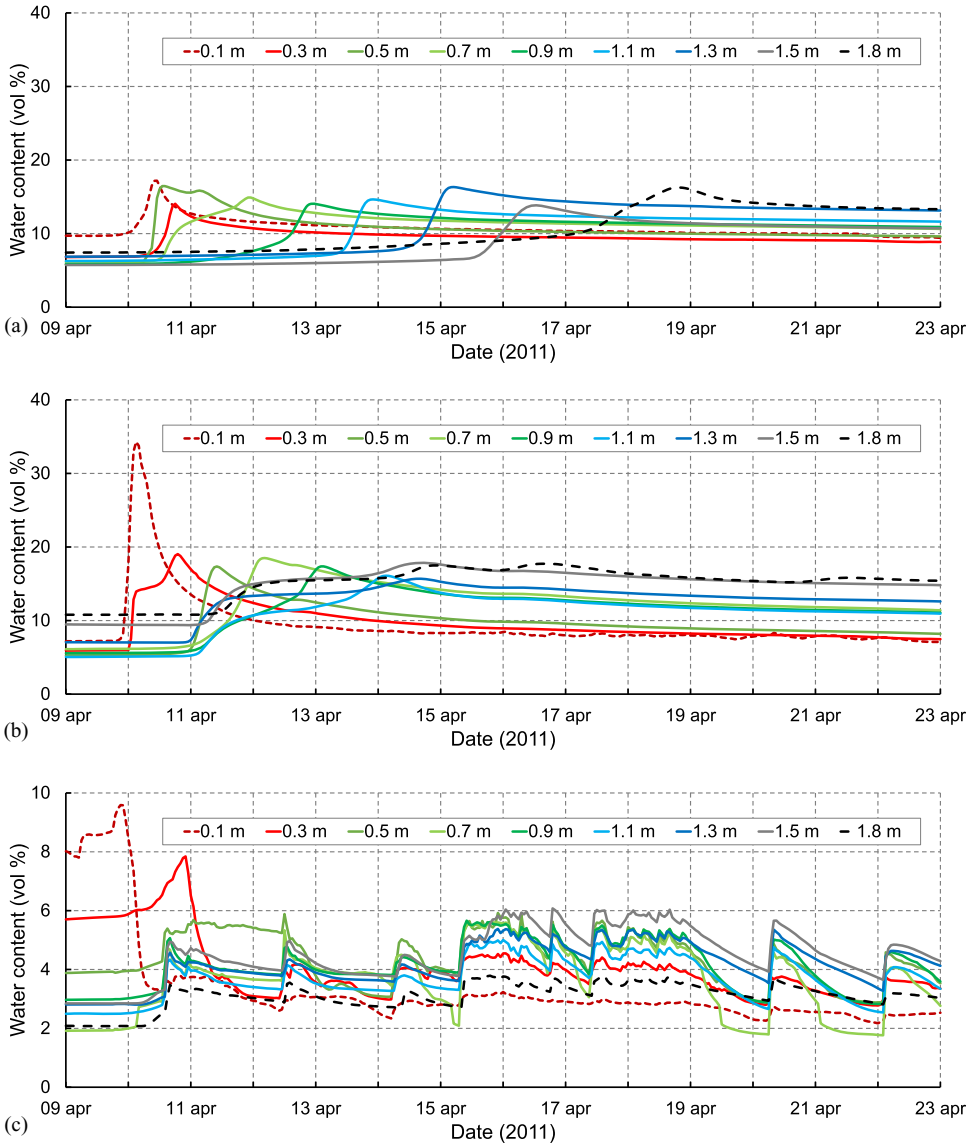

Fig. 6. (Color) Volumetric water content based on Sentek EnviroSCAN capacitance sensors in homogenous: (a) gravelly sand; (b) silty sand; and (c) 8–22 mm uniform, crushed gravel, April 2011.

Fig. 5 shows variations in volumetric soil water content for the period March 8–21, 2012, for three types of homogenous soils being thawed simultaneously. They are based on hourly readings from nine Sentek EnviroSCAN capacitance sensors. The sensor locations correspond to every second thermocouple, covering a 1.8 m soil column. Initially, before the heat load was applied and the soil started to thaw, the sensors reacted only to bound water, ranging from approximately 4–11 volume percent (vol%) in gravelly and silty sand to less than 5 vol% in uniform gravel. After the defroster was turned on, there was a short delay before the uppermost sensor (0.1 m) began responding to an increase in unbound water as pore ice started to melt. The rise in water content continued until a maximum level was reached, where all pore ice within the sensor's influence area had melted. As the thawing progressed further, excess water migrated downward with the thaw front, resulting in a sharp decrease in water content in the upper soil layer. The decline was more distinct for the sensors near the surface. In silty and gravelly sand, observed maximum levels down to 1.1 m were generally declining with increasing depth. From there and downward, maximum levels were either greater or equal to similar levels observed above 1.1 m depth.

The increase in unbound water at various depths down to 1.5 m in gravelly sand [Fig. 5(a)] occurred slightly earlier on the time axis compared with silty sand [Fig. 5(b)]. The time delay between responses at one depth compared with the next was nonlinear, that is, increased with depth. The exception was at 1.8 m, where the responses appeared to be occur at more or less the same time.

Soil water content in uniform gravel [Fig. 5(c)] was generally lower relative to gravelly and silty sand. The same sharp decrease after maximum level was reached was seen only at 0.1 m depth. The remaining sensors showed the water content stayed at maximum levels for gradually longer time periods before decreasing. For example, at 0.3 m depth, it stayed constant above 5 vol% for nearly 24 h, whereas at 0.7 m depth it remained at about 6 vol% for close to 6.5 days. The nonlinear increase in time between responses was considerably higher compared with the other soils.

The time needed for the sensors at 1.1 m depth to report having reached maximum water content after thawing was initiated is 89 h (3.7 days) in gravelly sand, 105 h (4.4 days) in silty sand, and 73 h (~3 days) in uniform gravel.

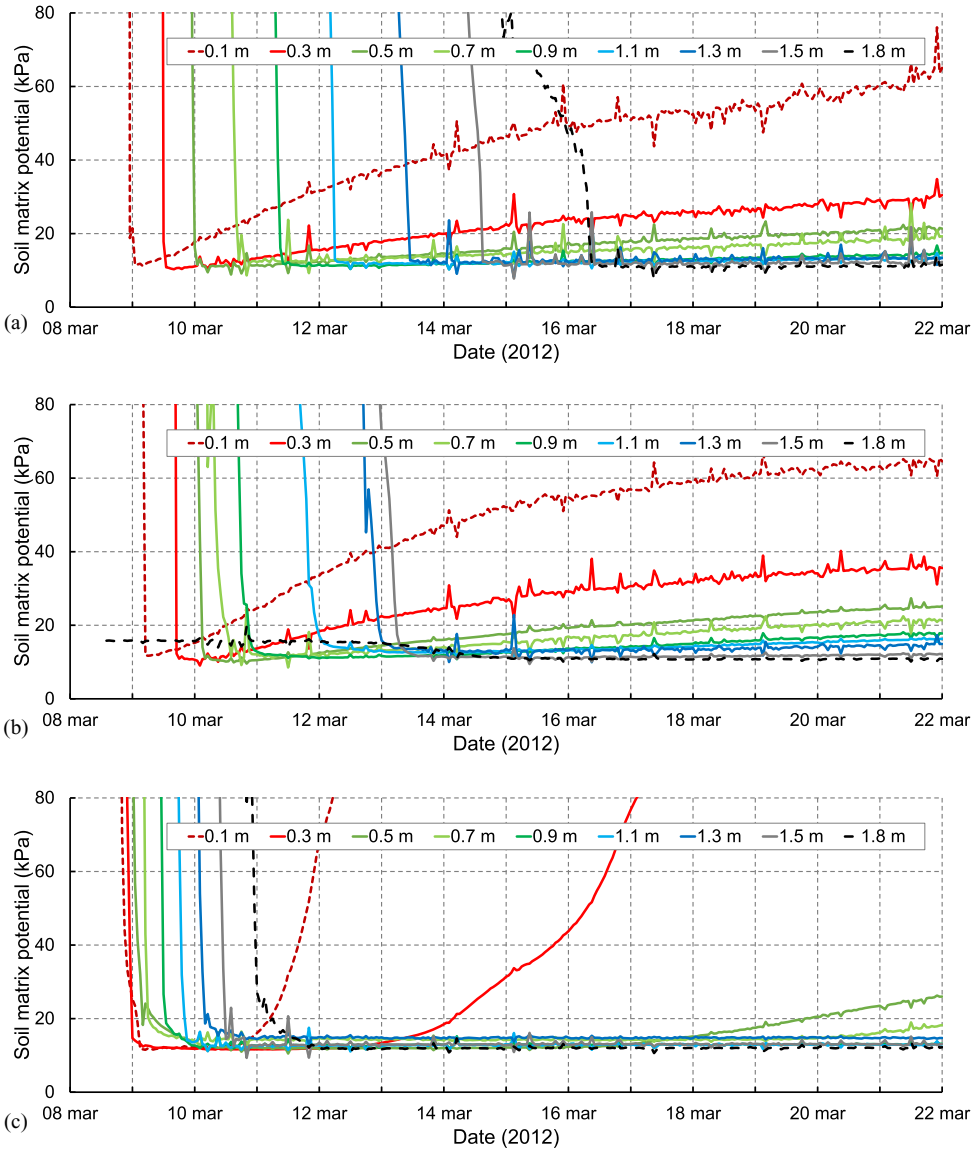

Fig. 7. (Color) Soil matrix potential (taken as positive values) based on Watermark 200SS electrical resistance records in homogenous: (a) gravelly sand; (b) silty sand; and (c) 8–22 mm uniform, crushed gravel, March 2012.

Similarly, Fig. 6 shows volumetric soil water records from April 9 to April 22, 2011 in the same soils, based on the same type of sensors and methodology as in 2012. As opposed to the temperature records, where data was missing for the initial 17 h, the soil moisture records are complete since they were collected by a separate data logging system. Generally, the soil moisture profiles differ from those in 2012. For example, when comparing the trends at 0.1–0.7 m depth in gravelly sand [Figs. 6(a) versus 5(a)] and at 0.5–1.8 m in silty sand [Figs. 6(b) versus 5(b)], the water content appeared to increase more or less simultaneously at the respective depths. There were also similarities, for example, initial water content and the levels after 12 days of thawing and onward were comparable.

In uniform gravel [Fig. 6(c)], initial water content down to about 0.9 m depth differed from similar content in 2012 [Fig. 5(c)]. Furthermore, maximum levels at 0.1 and 0.3 m depth were noticeably higher compared with 2011. Plus, the trends were markedly different. Those from 2011 were erratic throughout the experiment, alternately increasing and decreasing. Taken together with the near-simultaneous increase in water content at certain depths in gravelly and silty sand, this suggests that natural thawing had some influence on the experiments in 2011.

The time needed for the sensors at 1.1 m depth to reach maximum water content was 102 h (4.25 days) in gravelly sand, 107 h (~4.5 days) in silty sand, and 48 h (2 days) in uniform gravel. The latter refers to the first appearing maximum peak, while the actual maximum level for the whole time period appeared after 156 h (6.5 days).

Soil Matrix Potential

Figs. 7 and 8 show soil matrix potential (Ψ_m) based on electrical resistance records from March 8–21, 2012, and from April 10–22, 2011, respectively. The records are based on hourly readings from nine Watermark 200SS electrical resistance sensors at depths corresponding to the capacitance sensors. The manufacturers default calibration equation was used to determine Ψ_m, yielding results ranging from approximately −10 (wet) to more than −80 kPa (dry). In the current paper, Ψ_m is presented as positive values. For frozen soils being thawed, the high end of the scale (<80 kPa) is

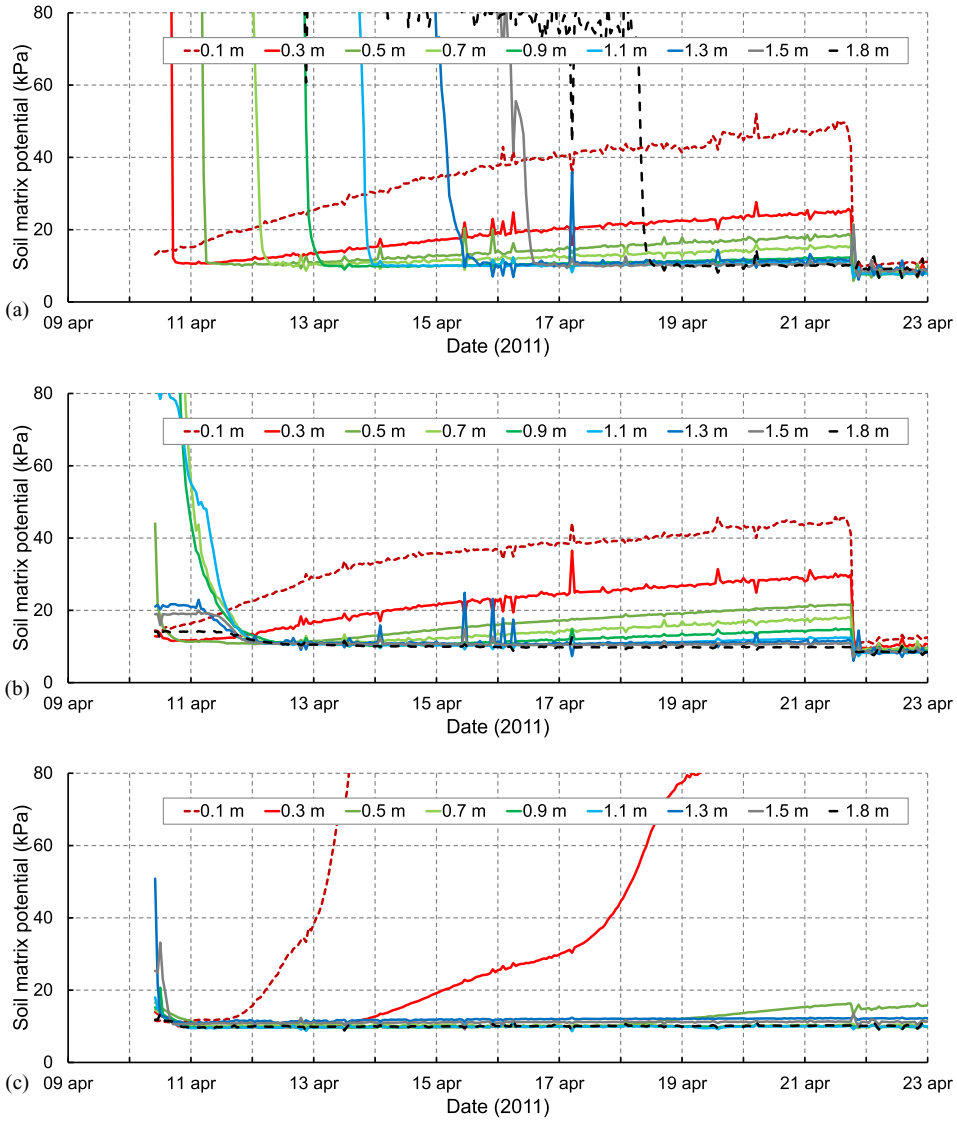

Fig. 8. (Color) Soil matrix potential (taken as positive values) based on Watermark 200SS electrical resistance records in homogenous: (a) gravelly sand; (b) silty sand; and (c) 8–22 mm uniform, crushed gravel, April 2011.

interpreted as frozen or partly frozen soil, whereas the low end (10–15 kPa) is taken as thawed soil. To avoid clutter, negative values or hysteresis in the resistance readings are removed. Furthermore, the results are temperature compensated based on soil temperature records (thermocouples) at depths corresponding to the resistance sensors. Consequently, Ψ_m cannot be determined for the initial 17 h for the experiment in 2011 (Fig. 8), since temperature records for that period were missing.

According to Shock et al. (1998), the calibration equation is developed specifically for the Watermark 200SS resistance sensor for soil matrix potentials ranging from −10 to −75 kPa, at soil temperatures between 15°C and 25°C, with reference to tensiometer readings. Thus, absolute Ψ_m-values presented are not accurate as occurring soil temperatures for the most part are lower than 15°C or substantially higher than 25°C. However, in this study it is the relative differences in time between minimum potentials occurring at various depths that are of interest, since they indirectly represent the dynamic (changing) status of the surrounding soil.

Referring to Fig. 7 in general, soil matrix potentials dropped abruptly to about 10–12 kPa in all three soils as the thawing progressed. In gravelly sand [Fig. 7(a)], the time between the drops increased gradually or nonlinearly, resembling the gradual time-delayed soil temperature response following phase changes. This was not the case in silty sand [Fig. 7(b)], where Ψ_m reached minimum levels comparatively earlier on the time axis, especially from 0.9 to 1.5 m depth. At 1.8 m, Ψ_m started low (15 kPa) and dropped only marginally (to 10 kPa) after one week of thawing, suggesting that the frost had not penetrated this deep at the time of the experiment in 2012.

Similar to silty sand, uniform gravel [Fig. 7(c)] differed from gravelly sand in that Ψ_m reached minimum considerably earlier on the time axis. For example, the sensor at 1.5 m depth reported the soil being thawed after approximately two days. According to the corresponding temperature records, the soil temperature was still lingering around zero at that time, suggesting that thawing (phase change) was still ongoing. Another distinction was a sharp increase in Ψ_m in the upper gravel layer during the experiment, noticeable at 0.1 and 0.3 m depths. The subsequent drop and erratic variations did not appear in the figure, since negative resistance values (hysteresis) are removed. The sharp increase and following rapid variations suggest ongoing freeze–thaw cycling in the upper gravel layer, and should not be confused with the

general or apparent increase in Ψ_m over time otherwise seen in gravelly and silty sand. The latter was a result of temperature compensation, where occurring soil temperatures were outside (above) the valid, upper limit.

The time needed for the sensors at 1.1 m depth to report wet or thawed conditions (10–15 kPa) was 88 h (3.7 days) in gravelly sand, 84 h (3.5 days) in silty sand, and 31 h (1.3 days) in uniform gravel.

Fig. 8 shows soil matrix potential variations from April 10 to 22, 2011, for the same soils, based on similar sensors and methodology as in 2012. In gravelly sand, the trends were not much different from those in 2012 [Figs. 8(a) versus 7(a)], although Ψ_m generally dropped to minimum levels slightly later in time. The nonlinear increase in time between drops suggests a somewhat lower thaw rate compared with the experiments in 2012. This is supported by corresponding soil temperature records for gravelly sand. For silty sand [Fig. 8(b)] and uniform gravel [Fig. 8(c)], the situation was opposite, with the resistance sensors reporting wet or thawed conditions much earlier on the time axis compared with 2012. For example, in silty sand at 0.7, 0.9 and 1.1 m depths, the decrease appeared to occur at more or less at the same time, approximately between 11 PM April 11 and 1 AM April 12. The same occurred at 1.3 m, even if the drop was less evident at this depth. In uniform gravel [Fig. 8(c)], the decrease occurred even earlier, again suggesting natural thawing affecting the experiment in 2011. Similar to 2012, the rapid increase and subsequent erratic variations at 0.1 and 0.3 m depths suggest ongoing freeze–thaw cycling in the upper gravel layer.

The effect of temperature compensation based on soil temperatures outside the valid range of the calibration equation can be found in the abrupt decrease in soil matrix potentials when the defroster was turned off and soil temperatures started dropping, after 6 PM April 21, shown in Figs. 8(a and b).

The time needed for the sensors at 1.1 m depth to report thawed soil was 103 h (4.3 days) in gravelly sand, 56 h (2.3 days) in silty sand, and approximately 22 h (∼1 day) in uniform gravel.

Discussion

The following sections discuss specific soils used and soil moisture records obtained during performance testing of the hydronic method in 2012 and 2011. Sensor output based on capacitance and electrical resistance are interpreted and assessed. Furthermore, ostensible characteristic water content variations resulting from artificial thawing based on hydronic heat are presented. Finally, thaw rates based on soil moisture records in the present paper are compared with thaw rates based on soil temperature records published in a previous paper (Sveen et al. 2016).

Soil Types Used

The soils used in the experiments were coarse-grained soils typically used when building foundations, pipe trenches, and road bases. In regions with seasonal or permafrost, soils such as silty sand would not see much use because of their high proportion of fines and consequently their susceptibility to frost. Nevertheless, they were included to complement the other two types of soil with regard to GSD and to ensure conformity with an initial experiment carried out in 2007 (Sveen and Sørensen 2010).

The soil samples in the bins are referred to as being homogenous. In context, that means being of the same type from the ground level down to 3 m depth, even though gradation range from smaller than 0.075 mm (fines) in silty sand up to 75 mm (cobbles) in gravelly sand. From Table 1, together with observed similarities in soil moisture and temperature trends, it appears that the soil composition of gravelly and silty sand could have been more diverse. Although the GSD curves suggest an adequate difference between the two, an even bigger proportion of fines in silty sand would increase its water susceptibility and thus its potential for standing out when being held up against gravelly sand.

Because the soil bins were exposed to the elements, seasonal as well as annual variations in soil moisture, ground-water table, ice content, and frost depths were expected. Even if these parameters were nearly the same from one winter to the next, they are of particular interest as the initial conditions decide the baseline for the experiments. Unfortunately, in this study, neither ground-water levels were monitored during the experiments nor initial ice content determined due to lack of access to suitable sampling equipment.

Soil Moisture Variations Based on Capacitance

Figs. 5 and 6 show what kind of spatial and temporal variations to expect in unbound water as pore ice changes phased in initially frozen soils subjected to hydronic heating. The figures cover two consecutive, identical thawing experiments, but where the first (in 2011) was affected by natural thawing. As the results are obtained by measuring the capacitance of the soil medium surrounding the sensors, and besides using a default calibration equation to correlate readings to volumetric water content, it is mainly relative differences that are of interest. It is assumed that the offset from the true level is more or less the same at all depths, thus allowing for direct comparisons, at least with regard to individual soils. Comparing dissimilar soils, however, relying on a single calibration equation may exaggerate differences in water content in cases where soils differ significantly in terms of type, texture, or gradation. In this study, gravelly and silty sand are considered close enough to allow for direct comparisons, both of initial water content levels prior to thawing, as well as maximum levels occurring during thawing.

Referring to Figs. 5(a and b), the frozen part of silty sand (down to about 1.4–1.5 m) contained slightly less or the same amount of bound water. As the soils started thawing, both the increase in unbound water and the observed maximum levels were higher in silty sand [Fig. 5(b)] compared with gravelly sand [Fig. 5(a)]. Uniform gravel [Fig. 5(c)] contained the least. This is reasonable considering the soils differed with regard to sand and fines content (Table 1), even though maximum at 0.1 m in gravelly sand exceeded that of silty sand at similar depths [Figs. 5(a) versus 5(b)]. A likely reason for the discrepancy is observed differences in ice layer thickness (3–6 cm) prior to the experiments. Supporting the assumption is the situation being opposite, or as expected, in 2011 [Figs. 6(a) versus 6(b)].

The amount of initially bound water is as expected compared with laboratory experiments on frozen silty loam performed by Wu et al. (2015). Earlier work by Williams (1964) demonstrated that fine-graded materials, such as silt and clays, could retain more than 50% (of dry weight) unfrozen water at soil temperatures just below zero. Even though this is far more than was observed in the current paper (note the difference in units), and besides both referring to fine-graded soils, they confirm that the bound water levels observed in this study are plausible.

For reference, Table 2 lists initial water content, maximum water content during thawing, and water content after 12 days of continuous thawing from 2012. Maximum levels for all soils down to about 1.1 m appeared to become less with increasing depth. Deeper down, levels were either higher or about equal compared with those above. The profiles presumably represent soil

Table 2. Bound (initial) and unbound (free) volumetric water content, based on capacitance sensors, 2012

Sensor location (m)	Volumetric water content (vol%)								
	Silty sand			Gravelly sand			Uniform gravel		
	init[a]	max[b]	12d[c]	init	max	12d	init	max	12d
0.1	6.4	24.5	6.3	8.2	34.1	9.2	3.6	6.5	2.2
0.3	6.1	19.3	7.4	6.0	16.6	8.8	3.5	5.6	2.2
0.5	5.0	16.8	8.2	5.4	15.0	9.6	4.6	6.7	2.7
0.7	5.3	16.5	11.4	5.5	12.7	10.6	3.8	6.4	1.8
0.9	4.9	15.8	10.8	5.5	12.9	11.2	3.3	5.2	3.7
1.1	4.2	14.4	10.3	5.7	13.0	11.8	2.2	3.4	3.2
1.3	4.9	16.1	11.3	6.1	14.8	13.3	2.6	3.9	3.5
1.5	5.7	18.8	14.4	5.1	12.7	11.1	2.3	3.8	3.2
1.8	10.5	17.7	15.6	6.6	15.7	13.6	1.6	2.7	2.2

Note: Sensor location refers to the depth at which the sensors are located, that is, the vertical distance from ground surface to the horizontal center-line of the sensors. The axial influence area are about 5 cm above and below this line, respectively.
[a]Initial water content in frozen soil.
[b]Maximum soil water content observed during thawing.
[c]Soil water content 12 days into the thawing experiment.

water status during natural freezing and should be noted for further investigation.

For all soils, the time-span from start thawing to just before the water content start dropping from maximum levels increased with depth. In gravelly sand, for example [Fig. 5(a)], the time-span between maximum at 0.1 and 0.3 m was 9 h, whereas similar between 0.3 and 0.5 m was 14 h, and so on. In silty sand [Fig. 5(b)], it was similar at 16 and 17 h, respectively. This corresponds to the nonlinear increase observed in soil temperature records from 2012, although capacitance sensors in gravelly sand respond slightly earlier as depth increases, relative to thermocouples. The drop from maximum levels at various depths was more pronounced in the upper layers, indicative of a larger degree of water redistribution and migration here. In uniform gravel [Fig. 5(c)], the situation was somewhat different in that maximum levels were reached earlier and stayed like that for increasingly longer durations with increasing depth, before eventually dropping. Presumably, this was owing to pore size, type, and structure in uniform gravel being significantly different relative to the other two soils, thus involving other moisture transport phenomena besides capillary transport.

Referring to Figs. 6(a and b), initial bound water and the following increase in unbound water were comparable to what was observed during the experiment in 2012, with the exception of uniform gravel [Fig. 6(c)]. However, a closer examination of the trends at 0.3–0.7 m in gravelly sand, and similar at 0.5–1.8 m depth in silty sand, showed a close to simultaneous increase in water content during thawing. This is typical for situations where the soils were thawed or partly thawed at the time of the experiment, where water migrates rapidly downward as the thawing progresses (Jabro et al. 2009). The same effect can be observed in the corresponding soil temperature records, although not that evident for the affected layers.

Since the experiment in 2011 was carried out one month later in the year and thus at the tail end of the normal cold season, natural thawing is likely to have started during the time leading up to the experiment. As 2011 was the first fieldwork season after establishing the FiG-lab, there are no soil temperature or moisture records prior to the experiment to support the assumption. Meteorological records from NMI show that there were in fact four warm spells, three of them combined with precipitation in the period from February 26 to March 21, 2011, which could explain the anomalies. Taking into account an 11-day period of frost leading up to the week prior to the experiments may also help explain why trends in uniform gravel [Fig. 6(c)] appeared so different from those in 2012. Apparently, the uppermost layer of uniform gravel started as thawed or partly thawed in 2011, whereas from approximately 0.7 m and below it was frozen. Subsequent erratic trends indicate parts of the gravel alternately refreezing and thawing during the experiment.

Soil Status Based on Electrical Resistance

Fig. 9 shows typical variations in electrical resistance down to 1.8 m depth in gravelly sand as it froze naturally during midwinter [Fig. 9(a)], and when it was artificially thawed throughout a two-week period in March 2012 [Fig. 9(b)]. The latter shows the type of data sets from which the soil matrix potentials were determined. In addition, associated soil temperatures were used to compensate for temperature variations. Consequently, the sharp decline in resistance to near zero at various depths corresponded exactly in time with when soil matrix potentials dropped to minimum [Figs. 9(b) versus 7(a)]. From Fig. 9(a) it appears as if the frost season came late that winter. However, the impression is misleading as the trends show frost penetration in only one type of homogenous (single-layered) soil, with the uppermost sensor embedded some distance below ground level. From similar trends in uniform gravel, supported by ambient air temperature records from NMI, it is clear that the cold season started as normal in early November 2011.

Due to space limitations, electrical resistances in silty sand and uniform gravel are not presented. However, Figs. 7 and 8 are compiled from the referred to resistance records, and they indirectly show that Watermark 200SS sensors misrepresented soil status in these particular soils during artificial thawing. Or more precisely, that they reported thawed conditions considerably earlier relative to Sentek capacitance sensors. The offset increased with depth. In fact, it was only in gravelly sand that responses from all four sensors types used, capacitance (Sentek EnviroScan), electrical resistance (Watermark 200SS), temperature (type T thermocouples), and thermistor strings (GeoPrecision), coincided in time. In the remaining soils, Watermark sensors disagreed with the others.

Spaans and Baker (1992) found that repeated calibration of selected Watermark 200 resistance blocks in the same soil produced different results and concluded that they were not suitable for accurate, reproducible measurements of soil matrix potential. Furthermore, they suggested that their use would be appropriate only for relative indications of soil wetness. Their assessment might have been different if they had access to the 200SS; an improved sensor version that came in the mid-1990s. Recent studies, both laboratory and field experiments (Chow et al. 2009; Chávez et al. 2011; El Marazky et al. 2011; Varble and Chávez 2011; Nolz et al. 2013; Rudnick et al. 2015), reported various degrees of success using Watermark 200SS sensors for determining soil matrix potential.

Suffice it to say, there are uncertainties attached to the electrical resistance data sets that reduce their utility value in this study. Although sensor- and soil-specific calibration would have provided better accuracy, further investigations are needed in order to identify possible reasons behind the observed discrepancies.

Soil Moisture Variations during Thawing

In Fig. 10, soil water content listed in Table 2 referring to thawing experiments in 2012 (blue) are presented as charts and compared

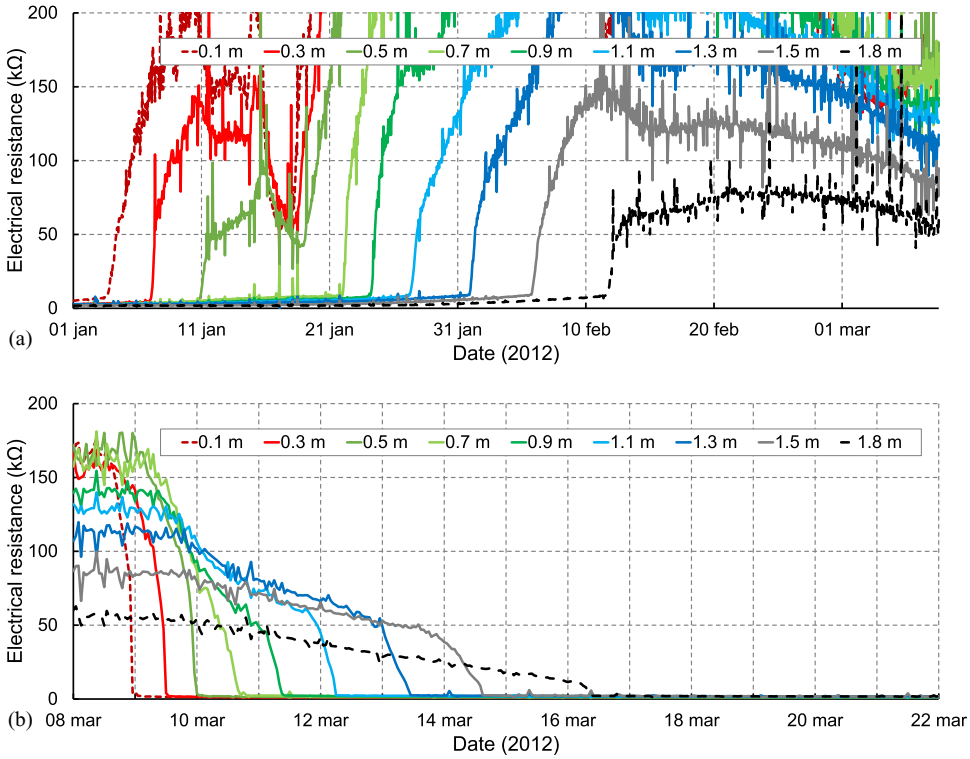

Fig. 9. (Color) Electrical resistance variations in homogenous gravelly sand: (a) January 1–March 8; and (b) March 8–22, both from 2012.

with similar thawing experiments conducted in 2011 (red). Initial (bound) water contents are excluded from the charts to maintain readability. Note that silty sand is presented before gravelly sand, as opposed to previous charts.

The dotted lines (labeled "$t = 12$ days") show the actual soil moisture profiles after 12 days of continuous thawing in 2012 and 2011, respectively. The continuous lines (labeled "maximum") show maximum soil water content observed during both thawing experiments, regardless of what time maximum occurred. As such, the maximum levels are not actual soil moisture profiles, but rather are an indicator of the redistribution and moisture migration taking place during artificial thawing. For example, referring to Fig. 10(a) and 2012 (blue lines), the volumetric water content at 5 cm depth had dropped from close to 25% early in the thawing process (continuous blue line), to approximately 6% after 12 days of thawing (dashed, blue line). A similar trend was observed in 2011 (red lines) at the same depth, although observed maximum level was higher, approximately 34%.

First, accounting for differences in dry density when comparing maximum volumetric water content during thawing (continuous lines) for all soils shown in Fig. 10, it followed that silty sand [Fig. 10(a)] contained more water than gravelly sand [Fig. 10(b)] and that uniform gravel [Fig. 10(c)] contained the least. This was the case for both experiments, acknowledging the previously noted discrepancy at 0.1 m depth between silty and gravelly sand. The results were as expected as soil water-holding capacity, among other factors, is related to amount and degree of fines and sand content (Table 1 and Fig. 4).

Second, the difference between maximum water content during thawing and water content after 12 days of thawing (dashed lines) showed that water redistribution and migration were more prominent in the uppermost layer for all soils. Taking into account a comparatively higher thaw rate close to the heat source, the downward movement of water was relatively fast initially. The trends were similar for both experiments, although differences observed in 2012 were generally slightly smaller compared with those in 2011.

Third, the profiles after 12 days of thawing showed a striking resemblance from one experiment to the next. In gravelly sand [Fig. 10(b)], for example, trends were close to identical from 0.3 to 1.8 m depth. This is somewhat surprising considering the site experienced changing weather conditions and snowpack in the period leading up to the experiments, as previously noted, supported by Table 3. Merely two data sets are not conclusive, but part of the explanation may be that the soil water-retention capacity of a certain soil composition is a basic property of said soil (Jabro et al. 2009).

Finally, from comparing the slopes of the profiles 12 days into thawing, it follows that silty sand held less water in the upper layer and more water in the lower layer than did gravelly sand. The slope in uniform gravel is close to vertical, indicating the water content being nearly the same in the entire soil profile. From maximum levels during thawing coinciding with levels after 12 days of thawing in 2012, it appears that the uniform gravel was still frozen below 1.1 m depth at that time of the experiment.

Thaw Rates Compared

Compared with similar experiments on artificial thawing of frozen ground, for example, (Oswell and Graham 1987; Lindroth et al. 1995; Hermansson and Guthrie 2006), unique for this study was simultaneously monitoring soil temperature and moisture responses during the process. In addition, two different measurement principles were utilized for measuring both parameters. Thermal responses and associated thaw rates were already known from the previous paper (Sveen et al. 2016). Therefore, a vital question was whether those thaw rates conformed to similar compiled from soil moisture records in the current paper. In Fig. 11, comparisons were made between thaw rates compiled from thermocouples

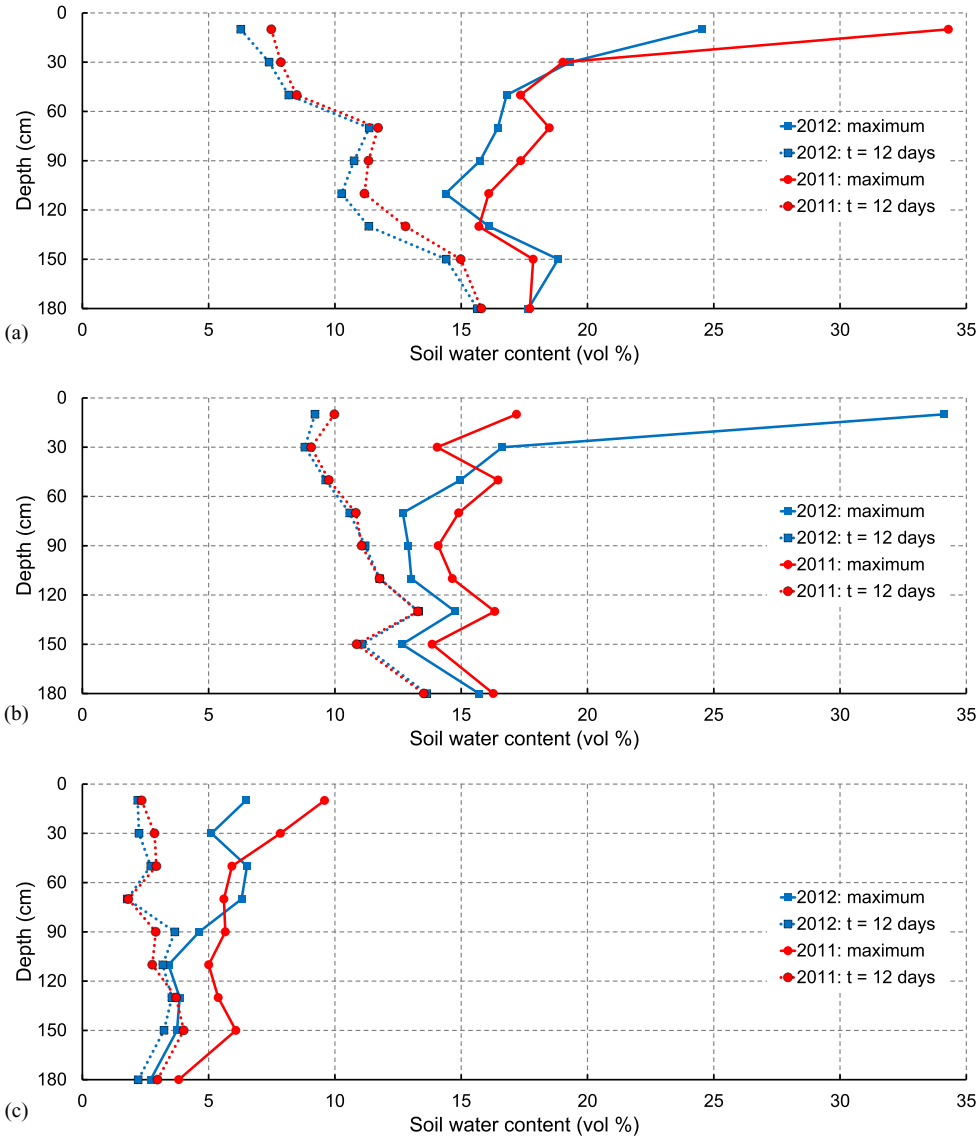

Fig. 10. (Color) Maximum volumetric soil water content observed during thawing ("maximum," continuous lines) and actual soil moisture profile after 12 days of thawing ("$t = 12$ days," dashed lines) of homogenous: (a) silty sand; (b) gravelly sand; and (c) 8–22 mm uniform, crushed gravel. Trends in 2011 (red, circle) versus 2012 (blue, square).

Table 3. Monthly mean air temperatures and precipitation in January–March 2012 and 2011, at Straumsnes Station, about 5.5 km east of the FiG-lab, 200 m above sea level

	Air temperature (°C)			Precipitation (mm)		
Month	2012	2011	Normal	2012	2011	Normal
January	–5.1	–4.6	–4.1	18	105	69
February	–5.2	–7.0	–3.9	77	51	64
March	–0.5	–1.9	–2.0	125	129	49

Note: "Normal" = Norwegian Meteorological Institute's 30-year average (1961–1990) in Narvik, Norway.

embedded in the soil and similar based on capacitance sensors in embedded access tubes. Records from 2011 were omitted because of natural thawing affecting the experiment.

Thaw rates compiled from soil temperatures were determined by calculating the time from start thawing to when there was a definite thermal response on the time axis. Close-ups of soil temperatures near zero degrees were evaluated individually for each depth and soil type. Similar calculations were made in this study, based on soil moisture response, determining the time from start thawing to when water contents started dropping from maximum levels. As capacitance sensor axial influence area extended 5 cm below its center-line (depth), corresponding thaw rates were displaced accordingly on the ordinate axis.

As shown in Fig. 11, thaw rates compiled from capacitance records correspond very well with similar based on soil temperature records for silty sand and uniform gravel. In silty sand [Fig. 11(a)], thaw rates were somewhat overestimated below 0.7 m depth, varying from 29 cm/day after one day (24 h) of thawing to approximately 25 cm/day after five days (120 h). In uniform gravel [Fig. 11(c)] the situation was the opposite, with rates slightly overestimated above 0.7 m, varying from 31 cm/day after one day of operation to approximately 13 cm/day after five days. In gravelly sand [Fig. 11(b)], capacitance sensors started overestimating thaw rates from about 0.3 m, increasing with depth. The difference is approximately 12 h at 1.0 m depth, and twice that at 1.5 m. Thaw rates here varied from 41 cm/day after one day to approximately 28 cm/day after five days.

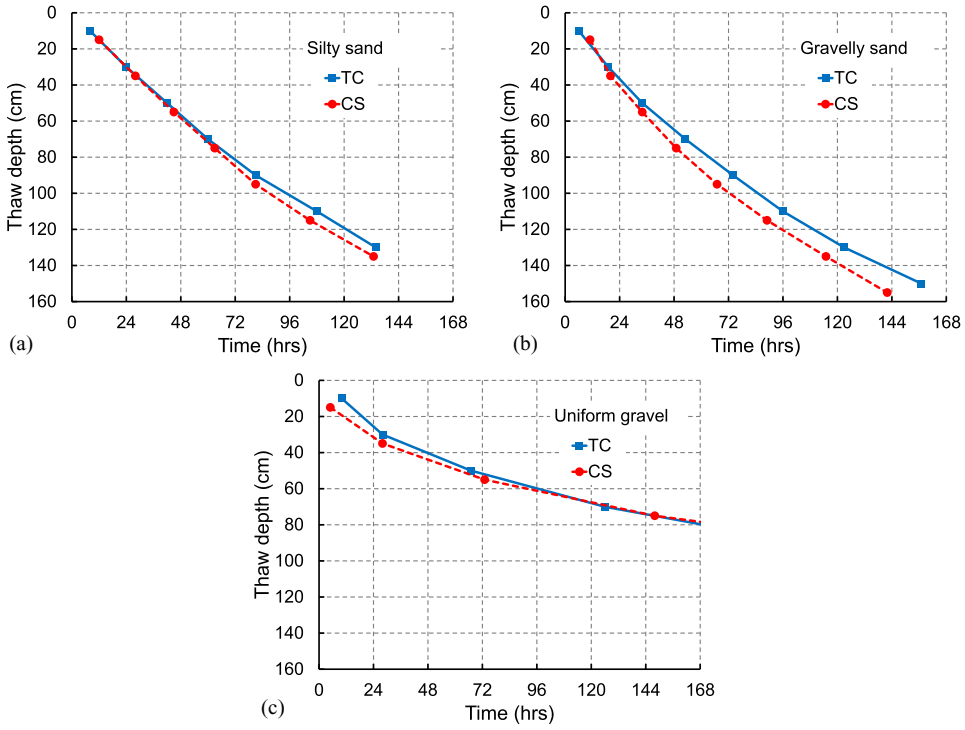

Fig. 11. (Color) Thaw depth versus time compiled from soil temperature (TC-thermocouples) and soil moisture records (CS-capacitance sensors) in (a) silty sand; (b) gravelly sand; and (c) 8–22 mm uniform, crushed gravel, March 2012.

Conclusion

Artificial thawing of initially frozen ground is about time-dependent heat and mass transfer in porous materials, where the total quantity of water that changes phase is one of the dominant factors affecting thaw rates. The current paper and the previous paper (Sveen et al. 2016) present the practical manifestation of those interconnected phenomena. Combined, the research provides thorough, scientific documentation of the hydronic thawing method in particular and a solid basis for further work.

An approach based on full-scale (in situ) experiments was chosen to obtain data necessary for assessing performance characteristics. Two identical experiments were carried out during the winters of 2011 and 2012, where hydronic heating was used to initiate and expedite the thawing process. The resulting spatial and temporal variations in soil temperature and moisture content were monitored simultaneously in three types of homogenous soils with varying ratio and amount of sand and fines content. In addition, two different measurement principles and appurtenant sensors were employed to measure each parameter.

Volumetric soil moisture content based on capacitance records from both experiments are presented, together with soil matrix potentials compiled from electrical resistance records. Some aspects of hydrodynamic behavior in frozen ground subjected to hydronic heating are emphasized, based on observed differences between water content during thawing (maximum) versus after a certain time period (12 days) of continuous thawing. Finally, thaw rates derived from soil moisture responses are presented and held up against similar compiled from soil temperature records. The following primary observations were obtained from this study:

1. Hydronic heating leads to a sharp increase in unbound water in the uppermost soil layer close to the heat source. Because artificial thawing is limited to small, confined areas, excess water becomes trapped, thus contributing to the thawing process.
2. The water content is higher and water redistribution and migration more prominent in soils with comparatively larger amounts and degree of fines and sand. For all soils examined, water redistribution is more evident in the uppermost layer.
3. Thaw rates compiled from soil moisture records correspond very well to similar based on soil temperature in silty sand and uniform gravel. In gravelly sand, capacitance sensors overestimate thaw rates from about 0.3 m depth. The offset increases with depth and amounts to approximately 12 h at 1.0 m.
4. Thaw rates decrease nonlinearly with increasing depth, ranging from 29 to 41 cm/day after one day of operation to 13–28 cm/day after five days of thawing.
5. Capacitance sensors are an excellent choice for evaluating relative differences in soil moisture content during artificial thawing. Quantitative analysis requires soil specific calibration.
6. Electrical resistance sensors may be suitable for monitoring soil status and determining soil matrix potentials in unfrozen soils, provided sensor and soil specific calibration. In frozen soils subjected to hydronic heating, the sensors misrepresent soil status, and drastically overestimate thaw rates under certain circumstances.

It is worth noting that the observations are based on two identical experiments, where the first (in 2011) was affected by natural thawing. Although meticulous planning and preparation went into ensuring comparable results from one season to the next, resultant uncertainties and limited scope warrant repeated experiments in order to fully assess the validity of the results presented.

Data Availability Statement

Some or all data, models, or code that support the findings of this study are available from the corresponding author upon reasonable request.

Acknowledgments

This study is funded by the Nordland County Council, the Cold-Tech Project (RT4-01), and Heatwork AS. The authors are grateful for the support in establishing the Frost in Ground laboratory (FiG-lab) and access to the facilities during this work. We would also like to thank Heatwork AS for providing the defrosting system used during the experiments.

References

Andersland, O. B., and B. Ladanyi. 2004. *Frozen ground engineering*. 2nd ed. Hoboken, NJ: Wiley.

Bäckström, M. 2000. "Ground temperature in porous pavement during freezing and thawing." *J. Transp. Eng.* 126 (5): 375–381. https://doi.org/10.1061/(ASCE)0733-947X(2000)126:5(375).

Baladi, J. Y., D. L. Ayers, and R. J. Schoenhals. 1981. "Transient heat and mass transfer in soils." *Int. J. Heat Mass Transf.* 24 (3): 449–458. https://doi.org/10.1016/0017-9310(81)90053-3.

Chávez, J. L., J. L. Varble, and A. A. Andales. 2011. "Performance evaluation of selected soil moisture sensors." In *Proc., 23rd Annual Central Plains Irrigation Conf.*, 29–38. Colby, KS: CPIA.

Chow, L., Z. Xing, H. W. Rees, F. Meng, J. Monteith, and L. Stevens. 2009. "Field performance of nine soil water content sensors on a sandy loam soil in New Brunswick, maritime region, Canada." *Sensors* 9 (11): 9398–9413. https://doi.org/10.3390/s91109398.

Drew, J. V., J. C. F. Tedrow, R. E. Shanks, and J. J. Koranda. 1958. "Rate and depth of thaw in Arctic soils." *Eos, Trans. Am. Geophys. Union* 39 (4): 697–701. https://doi.org/10.1029/TR039i004p00697.

El Marazky, M. S. A., F. S. Mohammad, and H. M. Al-Ghobari. 2011. "Evaluation of soil moisture sensors under intelligent irrigation systems for economical crops in arid regions." *Am. J. Agric. Biol. Sci.* 6 (2): 287–300. https://doi.org/10.3844/ajabssp.2011.287.300.

Esch, D. C. 2004. "Thermal analysis, construction, and monitoring methods for frozen ground." In Chap. 7 in *Thawing techniques for frozen ground*, edited by D. C. Esch, 239–257. Reston, VA: ASCE.

Evett, S. R., and J. L. Steiner. 1995. "Precision of neutron scattering and capacitance type soil water content gauges from field calibration." *Soil Sci. Soc. Am. J.* 59 (4): 961–968. https://doi.org/10.2136/sssaj1995.03615995005900040001x.

Guan, X. J., C. Spence, and C. J. Westbrook. 2010b. "Shallow soil moisture – ground thaw interactions and controls – Part 2: Influences of water and energy fluxes." *Hydrol. Earth Syst. Sci.* 14 (7): 1387–1400. https://doi.org/10.5194/hess-14-1387-2010.

Guan, X. J., C. J. Westbrook, and C. Spence. 2010a. "Shallow soil moisture – ground thaw interactions and controls – Part 1: Spatiotemporal patterns and correlations over a subarctic landscape." *Hydrol. Earth Syst. Sci.* 14 (7): 1375–1386. https://doi.org/10.5194/hess-14-1375-2010.

Heatwork. 2016a. "Areas of application." Accessed June 24, 2016. http://heatwork.com/en/areas-of-application/.

Heatwork. 2016b. "Products. technical data." Accessed June 24, 2016. https://heatwork.com/en/products/frostheater/technical-data/.

Hermansson, A., and W. S. Guthrie. 2006. "Numerical modeling of thaw penetration in Frozen ground subject to low-intensity infrared heating." *J. Cold Reg. Eng.* 20 (1): 4–19. https://doi.org/10.1061/(ASCE)0887-381X(2006)20:1(4).

Jabro, J. D., R. G. Evans, Y. Kim, and Iversen W. M. 2009. "Estimating in situ soil-water retention and field water capacity in two contrasting soil textures." *Irrig. Sci.* 27 (3): 223–229. https://doi.org/10.1007/s00271-008-0137-9.

Kurylyk, B. L., K. T. B. MacQuarrie, and C. I. Voss. 2014. "Climate change impacts on the temperature and magnitude of groundwater discharge from shallow, unconfined aquifers." *Water Resour. Res.* 50 (4): 3253–3274. https://doi.org/10.1002/2013WR014588.

Lindroth, D. P., W. R. Berglund, and C. F. Wingquist. 1995. "Microwave thawing of frozen soils and gravels." *J. Cold Reg. Eng.* 9 (2): 53–63. https://doi.org/10.1061/(ASCE)0887-381X(1995)9:2(53).

Myhre, Ø. (Ed.) 2010. *Frost in ground 2010*. Publ. No. 111. Oslo, Norway: Norwegian Public Roads Administration.

Nassar, I. N., R. Horton, and G. N. Flerchinger. 2000. "Simultaneous heat and mass transfer in soil columns exposed to freezing/thawing conditions." *Soil Sci.* 165 (3): 208–216. https://doi.org/10.1097/00010694-200003000-00003.

Nixon, J. F., and E. C. McRoberts. 1973. "A study of some factors affecting the thawing of frozen soils." *Can. Geotech. J.* 10 (3): 439–452. https://doi.org/10.1139/t73-037.

Nolz, R., G. Kammerer, and P. Cepuder. 2013. "Calibrating soil water potential sensors integrated into a wireless monitoring network." *Agric. Water Manage.* 116: 12–20. https://doi.org/10.1016/j.agwat.2012.10.002.

Oswell, J. M., and M. D. Graham. 1987. "Thawing frozen ground: Field trials and analysis." *J. Cold Reg. Eng.* 1 (2): 76–88. https://doi.org/10.1061/(ASCE)0887-381X(1987)1:2(76).

Paltineanu, I. C., and J. L. Starr. 1997. "Real-time soil water dynamics using multisensor capacitance probes: laboratory calibration." *Soil Sci. Soc. Am. J.* 61 (6): 1576–1585. https://doi.org/10.2136/sssaj1997.03615995006100060006x.

Rudnick, D. R., K. Djaman, and S. Irmak. 2015. "Performance analysis of capacitance and electrical resistance-type soil moisture sensors in a silt loam soil." *Trans. ASABE* 58 (3): 649–665. https://doi.org/10.13031/trans.58.10761

Shock, C. C., J. M. Barnum, and M. Seddigh. 1998. "Calibration of Watermark soil moisture sensors for irrigation management." In *Proc., 19th Annual Int. Irrigation-Association Techn. Conf.*, 139–146. Wuhan, China: Scientific Research.

Simonsen, E., and U. Isacsson. 1999. "Thaw weakening of pavement structures in cold regions." *Cold Reg. Sci. Technol.* 29 (2): 135–151. https://doi.org/10.1016/S0165-232X(99)00020-8.

Spaans, E. J. A., and J. M. Baker. 1992. "Calibration of Watermark soil moisture sensors for soil matric potential and temperature." *Plant Soil* 143 (2): 213–217. https://doi.org/10.1007/BF00007875.

Sveen, S., H. Nguyen, and B. Sørensen. 2016. "Thaw penetration in frozen ground subjected to hydronic heating." *J. Cold Reg. Eng.* 31 (1): 04016008. https://doi.org/10.1061/(ASCE)CR.1943-5495.0000117.

Sveen, S. E., and B. R. Sørensen. 2010. "Effective thawing of frozen ground – performance testing of a new thawing method based on hydronic heat." In *Proc. 3rd European Conf. on Permafrost*, 311. Svalbard, Norway: Univ. Centre in Svalbard.

Sveen, S. E., and B. R. Sørensen. 2013. "Establishment and instrumentation of a full scale laboratory for thermal and hygroscopic investigations of soil behavior in cold climates." *J Appl. Mech. Mater.* 239–240: 827–835. https://doi.org/10.4028/www.scientific.net/AMM.239-240.827.

Varble, J. L., and J. L. Chávez. 2011. "Performance evaluation and calibration of soil water content and potential sensors for agricultural soils in eastern Colorado." *Agric. Water Manage.* 101: 93–106. https://doi.org/10.1016/j.agwat.2011.09.007.

Wacker Neuson. 2016. "Hydronic surface heaters." Accessed November 6, 2016. http://www.wackerneuson.us/en/products/heaters/hydronic-surface-heaters/.

Williams, P. J. 1964. "Unfrozen water content of frozen soils and soil moisture suction." *Géotechnique* 14 (3): 231–246. https://doi.org/10.1680/geot.1964.14.3.231.

Wu, M., X. Tan, J. Huang, J. Wu, and P. E. Jansson. 2015. "Solute and water effects on soil freezing characteristics based on laboratory experiments." *Cold Reg. Sci. Technol.* 115: 22–29. https://doi.org/10.1016/j.coldregions.2015.03.007.

Xu, H., and J. D. Spitler. 2014. "The relative importance of moisture transfer, soil freezing and snow cover on ground temperature predictions." *Renewable Energy* 72: 1–11. https://doi.org/10.1016/j.renene.2014.06.044.

Yang, M. X., T. D. Yao, X. H. Gou, T. Koike, and Y. Q. He. 2003. "The soil moisture distribution, thawing–freezing processes and their effects on the seasonal transition on the Qinghai–Xizang (Tibetan) plateau." *J. Asian Earth Sci.* 21 (5): 457–465. https://doi.org/10.1016/S1367-9120(02)00069-X.